doi:10.1038/nature07725

LETTERS

AIM2 recognizes cytosolic dsDNA and forms a caspase-1-activating inflammasome with ASC

Veit Hornung[1,2], Andrea Ablasser[1,2], Marie Charrel-Dennis[1], Franz Bauernfeind[1,2], Gabor Horvath[1], Daniel. R. Caffrey[3], Eicke Latz[1]* & Katherine A. Fitzgerald[1]*

The innate immune system senses nucleic acids by germline-encoded pattern recognition receptors. RNA is sensed by Toll-like receptor members TLR3, TLR7 and TLR8, or by the RNA helicases RIG-I (also known as DDX58) and MDA-5 (IFIH1)[1]. Little is known about sensors for cytoplasmic DNA that trigger antiviral and/or inflammatory responses[2–6]. The best characterized of these responses involves activation of the TANK-binding kinase (TBK1)–interferon regulatory factor 3 (IRF3) signalling axis to trigger transcriptional induction of type I interferon genes[2,3]. A second, less well-defined pathway leads to the activation of an 'inflammasome' that, via caspase-1, controls the catalytic cleavage of the pro-forms of the cytokines IL1β and IL18 (refs 6, 7). Using mouse and human cells, here we identify the PYHIN (pyrin and HIN domain-containing protein)[8] family member absent in melanoma 2 (AIM2) as a receptor for cytosolic DNA, which regulates caspase-1. The HIN200 domain of AIM2 binds to DNA, whereas the pyrin domain (but not that of the other PYHIN family members) associates with the adaptor molecule ASC (apoptosis-associated speck-like protein containing a caspase activation and recruitment domain) to activate both NF-κB and caspase-1. Knockdown of *Aim2* abrogates caspase-1 activation in response to cytoplasmic double-stranded DNA and the double-stranded DNA vaccinia virus. Collectively, these observations identify AIM2 as a new receptor for cytoplasmic DNA, which forms an inflammasome with the ligand and ASC to activate caspase-1.

Our current understanding of the mechanisms sensing cytoplasmic DNA is limited[9]. A candidate receptor called DAI (DNA-dependent activator of interferon (IFN)-regulatory factors) has been implicated in the DNA-induced type I IFN pathway[4]. The NLR family member NLRP3 has also been shown to activate caspase-1 in response to internalized adenoviral DNA[6]. Caspase-1 activation in response to transfected bacterial, viral, mammalian or synthetic DNA, however, does not involve NLRP3, although the adaptor molecule ASC is required[6,7].

We proposed that an upstream activator of this double-stranded DNA (dsDNA)-activated ASC pathway would contain a pyrin domain (PYD) for homotypic interaction with ASC, and at least one other domain for direct binding to DNA or for association with an upstream receptor. In addition to NLRP3 (ref. 10), NLRP6 (ref. 11) and NLRP12 (ref. 12) have previously been shown to associate with ASC. Although ASC-deficient macrophages failed to activate caspase-1 and trigger IL1β release in response to poly(dA-dT) • poly(dA-dT) (hereafter referred to as poly(dA:dT))[2], macrophages lacking NLRP3, NLRP6 and NLRP12 responded normally (Fig. 1a). Surprisingly, we found that macrophages lacking ASC produced higher levels of IFNβ and IL6 in response to poly(dA:dT), which was not observed in cells lacking NLRP3, the IL1 receptor, or to a lesser extent caspase-1 (Supplementary Fig. 1a–d). Poly(dA:dT)-induced cell death also occurred in an ASC-dependent manner (Supplementary Fig. 1e, f). We speculate that the increased cytokine production in ASC-deficient cells relates to their resistance to poly(dA:dT)-induced cell death. In addition to poly(dA:dT), dsDNA from natural sources activated caspase-1 cleavage (Supplementary Fig. 2a, b). In contrast, a small immunostimulatory oligonucleotide[3], long single-stranded DNA (ssDNA; poly(dI)), transfected dsRNA or the ssRNA virus Sendai virus failed to trigger this response in *Nlrp3*-deficient macrophages (Supplementary Fig. 2c).

Searching the PFAM database[13] we identified several PYD-domain containing proteins, which also contained a HIN200 domain, previously shown to bind DNA[14]. In humans, the HIN200 family consists of four members[15]: IFIX (also known as PYHIN1)[16], IFI16 (ref. 17), MNDA[18] and AIM2 (ref. 19). A multiple-sequence alignment of PYD domains from these proteins with PYD domains from some of the NLR proteins is shown in Fig. 1b. Sequence analysis of IFIX, IFI16 and MNDA predicted their nuclear localization, in contrast to AIM2, which was predicted to be cytosolic (Fig. 1c, bottom panel). Consistent with these predictions, fluorescent protein chimaeras of IFIX, IFI16 and MNDA localized to the nucleus, whereas AIM2 was almost exclusively cytoplasmic (Fig. 1d).

To study the possibility that these PYHIN proteins associated with ASC, we generated carboxy-terminally tagged PYD–CFP (cyan fluorescent protein)-domain fusions (which lacked the putative nuclear localization sequences identified above). Indeed, all of the PYD–CFP fusions were localized to the cytoplasm (Supplementary Fig. 3). To test whether induced clustering of the PYD–CFP fusions led to association with ASC–YFP (yellow fluorescent protein), we used a human embryonic kidney 293 cell line that stably expressed ASC–YFP at low enough levels to be polydispersed throughout the cytoplasm (Fig. 2a, mock). Indeed, overexpression of the NLRP3–CFP-tagged PYD domain led to the formation of large cytosolic aggregates, which co-aggregated with ASC–YFP (Fig. 2a). Notably, in most transfected cells, extensive intracellular co-localization with ASC–YFP was observed with a complete loss of the cytoplasmic distribution of ASC–YFP[10,11,20]. Of all the PYHIN-PYD proteins tested, only AIM2-PYD led to complex formation with ASC (Fig. 2a, b and Supplementary Fig. 4). Similar results were obtained with full-length AIM2–CFP but not with full-length IFIX, IFI16 or MNDA, which were all localized to the nucleus (Fig. 2a, b and Supplementary Fig. 5a, b). Additionally, only AIM2-PYD and NLRP3-PYD were found to bind haemagglutinin (HA)-tagged ASC in co-immunoprecipitation studies (Fig. 2c). Furthermore, endogenous ASC associated with endogenous AIM2, but not with IFI16 in primed THP-1 cells (Fig. 2d).

[1]Division of Infectious Diseases and Immunology, Department of Medicine, University of Massachusetts Medical School, Worcester, Massachusetts 01605, USA. [2]Institute of Clinical Chemistry and Pharmacology, Universitätsklinikum Bonn 53127, Germany. [3]Pfizer, 620 Memorial Drive, Cambridge, Massachusetts 02139, USA.
*These authors contributed equally to this work.

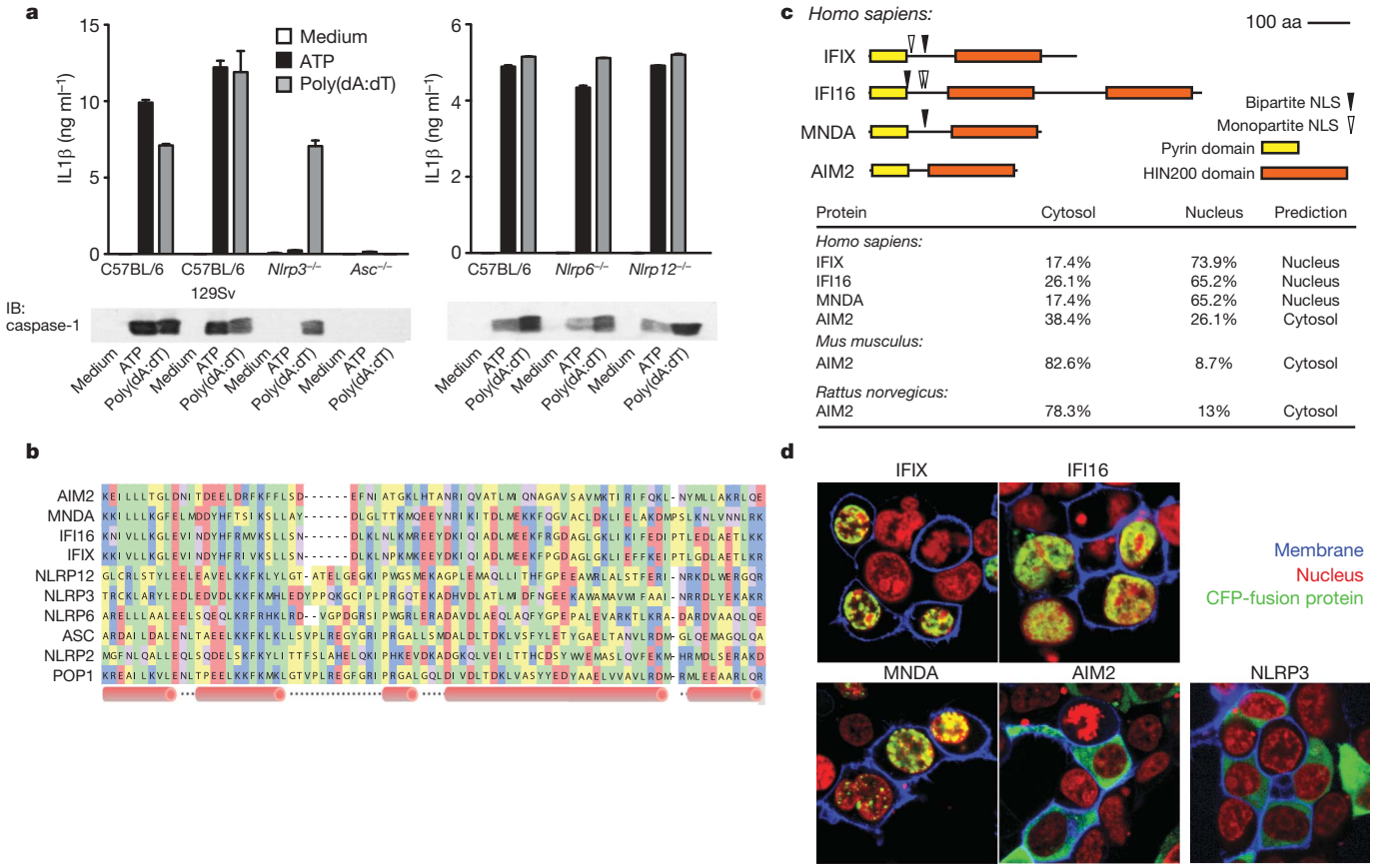

Figure 1 | Poly(dA:dT)-induced inflammasome activation. **a**, LPS-primed macrophages from wild type or inflammasome-deficient mice were stimulated as indicated and supernatants were examined for IL1β by ELISA or for cleaved caspase-1 by immunoblot. Error bars represent s.d. **b**, A multiple-sequence alignment of human PYHIN and select NLR PYD domains. **c**, Domain structures of human PYHINs, with predicted nuclear localization signals and subcellular localizations (bottom panel). aa, amino acids; NLS, nuclear localization sequence. **d**, Subcellular localization of CFP-tagged IFIX, IFI16, MNDA, AIM2 or NLRP3 (all green) in 293T cells. Fluorescent cholera-toxin-stained membranes (blue) and DRAQ5-stained nuclei (red). Original magnification, ×150. Data from one experiment of three is shown (**a**, **d**).

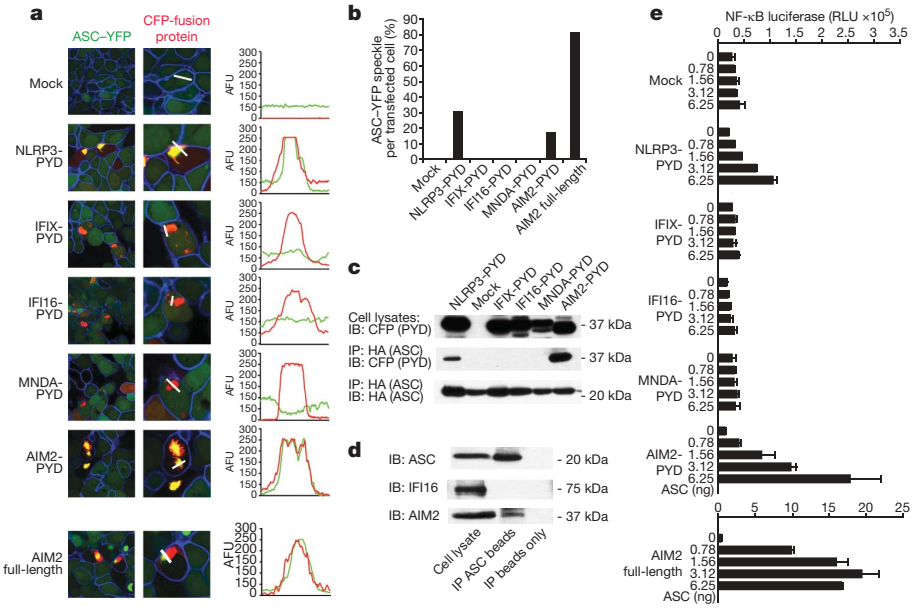

Figure 2 | AIM2 interacts with ASC. **a**, ASC–YFP-expressing cells (green) were transfected as indicated and imaged by confocal microscopy. Original magnification, ×150. AFU, arbitrary fluorescent units. **b**, The fluorescence intensities of green (ASC–YFP) and red (PYD–CFP) channels were quantified along the white lines in **a** and the percentage of ASC–YFP speckles was calculated. **c**, 293T cells transfected with HA–ASC and CFP-tagged constructs as in **a** were immunoprecipitated (IP) with an anti-HA antibody and immunoblotted (IB) as indicated. **d**, ASC was immunoprecipitated from Sendai-virus-primed THP-1 cells, and ASC, IFI16 and AIM2 were examined by immunoblotting. The band above the AIM2 band in the ASC immunoprecipitation corresponds to the heavy chain of the anti-ASC antibody. **e**, NF-κB luciferase reporter gene activity was measured on transfection with the indicated plasmids. Data are representative of one experiment out of three (**a**–**d**) or out of two (**e**). Error bars, s.d.

To examine the functional relevance of AIM2–ASC complex formation, we examined NF-κB reporter gene activity in cells overexpressing the PYHIN-PYD proteins in the presence of ASC. Only NLRP3-PYD and AIM2-PYD led to potent NF-κB activation (Fig. 2e). The effect of full-length AIM2 was even more marked (Fig. 2e, bottom panel). The full-length versions of IFIX, IFI16 and MNDA failed to activate NF-κB (Supplementary Fig. 5c). ASC was absolutely required, because no substantial NF-κB reporter activity was observed in cells not transfected with ASC. No substantial activation of the IFNβ promoter reporter gene was observed with any of the PYHIN family members (Supplementary Fig. 6).

We next examined whether the AIM2–ASC complex could lead to the formation of a functional inflammasome complex and caspase-1-dependent maturation of pro-IL1β. We used a transient transfection assay overexpressing the respective proteins of interest in the presence of ASC, caspase-1 and Flag-tagged pro-IL1β in 293T cells and monitored the cleavage of pro-IL1β by immunoblotting. Among the PYD proteins tested, only NLRP3-PYD and AIM2-PYD induced maturation of pro-IL1β, when ASC and caspase-1 were co-expressed (Fig. 3a). Full-length AIM2 was even more potent than AIM2-PYD (Fig. 3a, lower panel). Neither the PYD domain nor the full-length versions of IFIX, IFI16 or MNDA induced IL1β cleavage (Supplementary Fig. 7).

To study the role of AIM2 in cells with a functional poly(dA:dT)-triggered or dsDNA-virus-induced inflammasome complex, we used lentiviruses encoding short hairpin RNAs (shRNAs) to knock down *Aim2* in immortalized murine macrophage cell lines (B6-MCLs or N3-KO-MCLs)[7]. AIM2 was expressed constitutively both in primary macrophages and in B6-MCLs, and was further induced by poly(dA:dT) or Sendai virus (Supplementary Fig. 8). Three different shRNAs were tested, of which two (*Aim2* shRNA2 and shRNA3) resulted in a strong reduction of *Aim2* expression (Fig. 3b). Knocking down *Aim2*, but not an unrelated gene, resulted in a strong attenuation of both poly(dA:dT)-mediated IL1β release (Fig. 3c) and caspase-1 cleavage (Fig. 3d). Targeting human *AIM2* in THP-1 cells using short interfering RNA (siRNA) corroborated these findings (Supplementary Fig. 8d, e). Moreover and consistent with what we had seen in ASC-deficient macrophages (Supplementary Fig. 1), knocking down *Aim2* resulted in a marked enhancement of poly(dA:dT)-mediated type I IFN induction (Supplementary Fig. 8b). This effect was specific because the IFNβ response to Sendai virus was unaffected (Supplementary Fig. 8c). Furthermore, in agreement with the results obtained in ASC-deficient macrophages, macrophages that were targeted with *Aim2* shRNAs were resistant to poly(dA:dT)-triggered cell death (Fig. 3e). We also examined the role of AIM2 in the recognition of the dsDNA vaccinia virus. Similar to what we had observed with transfected poly(dA:dT), vaccinia-virus-induced caspase-1 cleavage occurred in an ASC-dependent but an NLRP3-independent manner (Fig. 3f). This effect was also dependent on AIM2, because shRNA-mediated knockdown of *Aim2* impaired vaccinia-virus-induced caspase-1 cleavage but not that induced by anthrax lethal toxin (Fig. 3g). Knockdown of a control protein did not affect caspase-1 cleavage after vaccinia virus infection. Vaccinia-virus-triggered cell death was also strongly reduced in *Aim2*-shRNA-targeted macrophages, but not in control macrophages (Fig. 3h). Altogether, these results indicated that AIM2 controlled inflammasome activation and cell death in response to dsDNA and the dsDNA vaccinia virus.

To determine whether AIM2 could be involved in the recognition of dsDNA directly, we generated fluorescein-labelled poly(dA:dT), (FITC-DNA), and co-transfected FITC-DNA together with CFP-tagged versions of full-length AIM2, AIM2-HIN, AIM2-PYD or full-length NLRP3. Whereas cells expressing NLRP3 or AIM2-PYD showed no co-localization of the respective proteins with FITC-DNA, full-length AIM2 and AIM2-HIN showed extensive co-localization with FITC-DNA and led to the formation of DNA and protein aggregates in the cytosol (Fig. 4a). We used single cell flow cytometry fluorescence resonance energy transfer (FRET) measurements to quantify these interactions (Fig. 4b)[21]. A dose-dependent increase in FRET between full-length AIM2 and FITC-DNA was seen, whereas AIM2-PYD did not lead to measurable FRET. Other proteins such as NLRP3 and IFI16 did not show any FRET (data not shown).

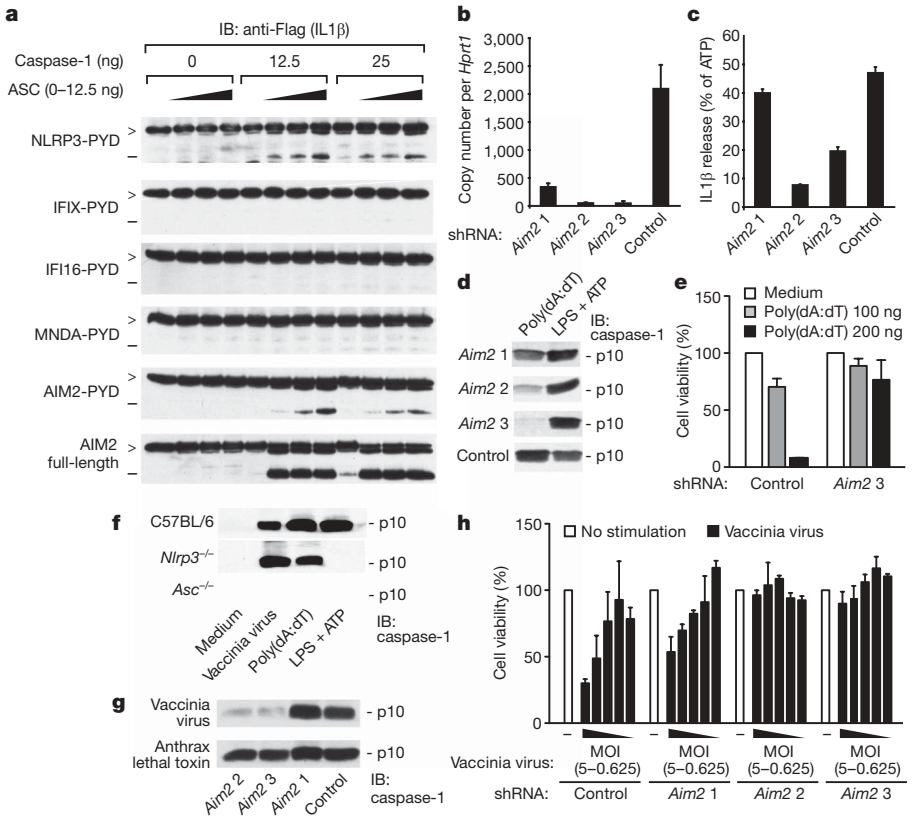

Figure 3 | AIM2 is required for poly(dA:dT)- and vaccinia-virus-triggered inflammasome activation. **a**, 293T cells were transfected as indicated and the cell lysates were immunoblotted for pro-IL1β (>) and cleaved IL1β (−). **b**, B6-MCLs were transduced with lentiviral vectors encoding shRNAs as indicated, and *Aim2* and *Hprt1* were measured by quantitative rtPCR. **c**, LPS-primed cells as in **b** were stimulated as indicated for 6 h and IL1β in the supernatants was measured by ELISA. The poly(dA:dT)-triggered IL1β release was normalized to the ATP-induced IL1β levels. Absolute values for ATP-triggered IL1β release were 1,790, 2,078, 2,676 and 1,119 pg ml^{-1} for *Aim2* shRNA1, shRNA2, shRNA3 and control, respectively. **d**, Macrophages as in **b** were treated as indicated, and the cleavage of caspase-1 was measured by immunoblotting after 6 h. **e**, Macrophages transduced with shRNA were transfected as indicated and cells were counted 24 h later. **f**, Macrophages from the indicated strains were treated as indicated and cleavage of caspase-1 was measured after 6 h. **g**, *Nlrp3*-deficient shRNA-expressing macrophages as in **b** were infected as indicated and assessed for cleavage of caspase-1 after 6 h. **h**, Cells as in **b** were infected as indicated and cell survival was measured by calcein AM staining 24 h later. MOI, multiplicity of infection. One representative experiment out of three (**a**, **d**–**h**), four (**c**) or five (**b**) is depicted. Error bars represent s.d.

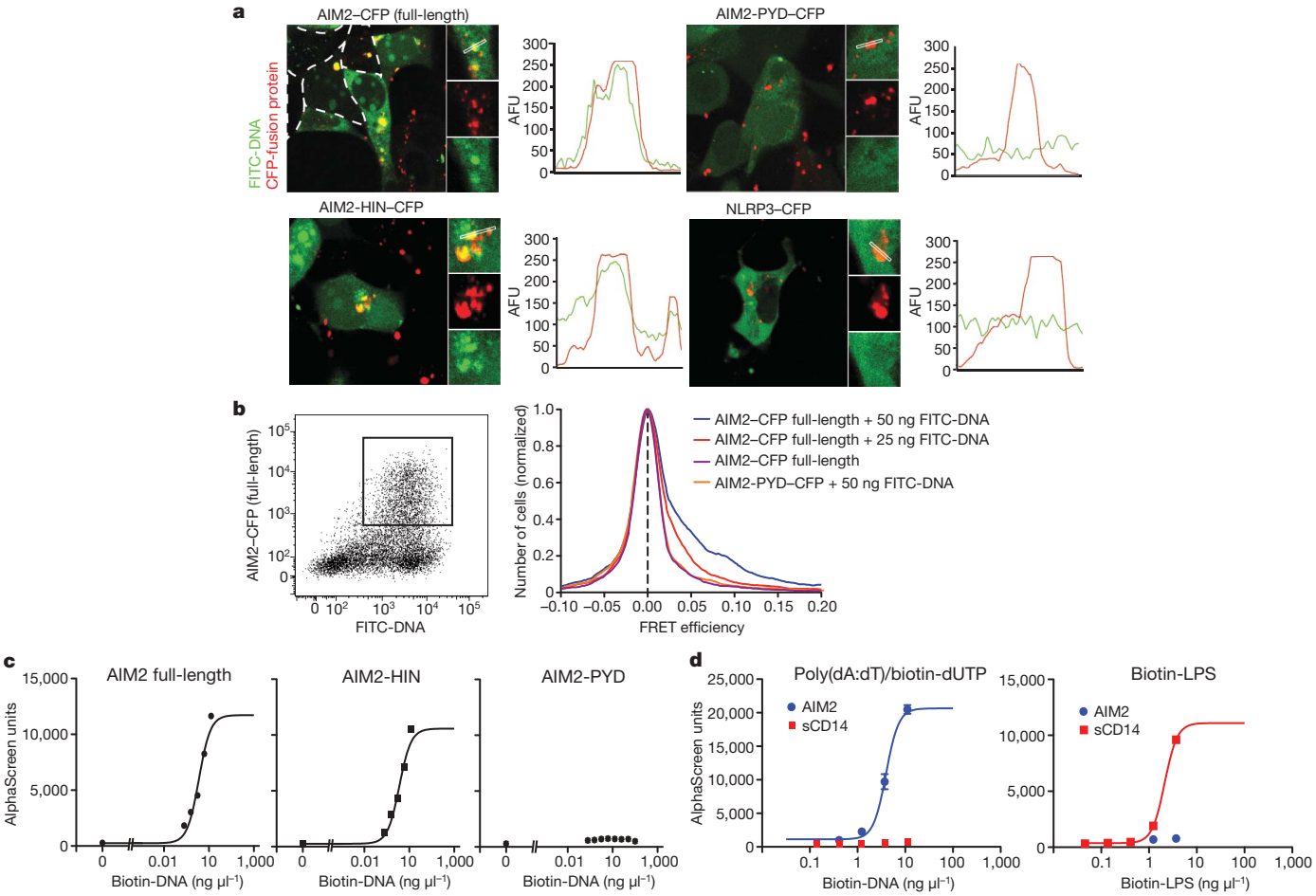

Figure 4 | AIM2 binds dsDNA via its HIN domain. a, 293T cells were transfected with CFP-tagged AIM2 or NLRP3 (both red) as indicated, together with FITC-DNA (green), and imaged by confocal microscopy. Fluorescence intensities of the green (FITC-DNA) and red (CFP-fusion protein) channels were quantified along selected lines. Original magnification, ×150. **b**, 293T cells were transfected as indicated with FITC-DNA or unlabelled DNA. Cells were analysed by flow cytometry after 24 h and CFP- and FITC-positive cells were gated (left panel) and analysed for FRET efficiency on a cell-by-cell basis. Calculated FRET efficiency histograms are shown (right panel). **c**, **d**, AlphaScreen assessment of AIM2 full-length, AIM2-HIN or AIM2-PYD binding to poly(dA:dT)/biotin-dUTP (biotin-DNA) (**c**) and AIM2 or soluble CD14 (sCD14) binding to biotin-DNA or biotin-LPS (**d**). Representative data from two (**d**) or three (**a**–**c**) independent experiments are shown.

Furthermore, binding studies using purified AIM2, AIM2-HIN and AIM2-PYD with biotinylated poly(dA:dT) (biotin-DNA) showed that AIM2 directly interacted with poly(dA:dT) with high affinity; only full-length AIM2 or the AIM2-HIN was able to bind biotin-DNA (Fig. 4c). Binding of poly(dA:dT) to AIM2 was specific, because AIM2 did not bind biotin-lipopolysaccharide (LPS), which bound to soluble CD14 under similar assay conditions (Fig. 4d).

Collectively, these data identify AIM2 as a receptor for cytosolic dsDNA, which forms a new inflammasome complex with ASC to activate caspase-1-mediated processing of IL1β. Our data also indicate that the activation of the AIM2 inflammasome is important in innate immunity to vaccinia virus. Because bacterial pathogens such as *Francisella tularensis*[22] and aberrant host DNA in pathological autoimmunity[23] also trigger the IL1β pathway, it will be important to define the role of AIM2 in these responses. Further characterization of the AIM2 inflammasome as a sensor of microbial, as well as host DNA, may therefore enable the rational design of new therapies and treatments for infectious as well as autoimmune diseases.

METHODS SUMMARY

Reagents and mice. All complementary DNAs were cloned by PCR from cDNA into pEFBOS-C-term-CFP and subcloned into pEFBOS-C-term-Flag/His. Biotinylated and FITC-labelled poly(dA:dT) were made by adding biotin-dUTP or FITC-dUTP (Fermentas) at a molar ratio of 1:8 to dTTP in the enzymatic synthesis of poly(dA:dT) as described[24]. Vaccinia virus (Western Reserve strain) was from K. Rock. The anti-human AIM2 antibody (3B10) was from R. Johnstone. *Nlrp3*$^{-/-}$ and *Pycard*$^{-/-}$ mice were as previously described[25]. Both strains, as well as *NlrP6*$^{-/-}$ and *Nlrp12*$^{-/-}$ mice, were from Millennium Pharmaceuticals. Caspase-1-deficient mice were from R. Flavell. *Il1r1*$^{-/-}$ mice were from Jackson Laboratories.

Bone-marrow-derived macrophages were stimulated as indicated. Poly(dA:dT) DNA and all other DNAs were transfected using Lipofectamine 2000 at a concentration of 1 µg ml^{-1}. Cell culture supernatants were assayed for IL1β using ELISA kits from BD Biosciences. Confocal microscopy was performed on a Leica SP2 AOBS confocal laser scanning microscope. FRET efficiencies were calculated on a cell-by-cell basis[21] and histograms were plotted with GraphPad Prism 5.01 (GraphPad Software). Immunoblot analysis was conducted as previously described[7]. Quantitative real-time PCR (rtPCR) analysis was performed as previously described[26]. Lentiviral shRNAs targeting *Aim2* were obtained from OpenBiosystems and shRNA silencing was carried out as described (http://www.broad.mit.edu/genome_bio/trc/publicProtocols.html). The AlphaScreen (amplified luminescent-proximity homogeneous assay) was set up as an association assay and read with the Envision HT microplate reader (Perkin Elmer). Reporter assays for NF-κB or IFN luciferase reporters were carried out as previously described[26].

Full Methods and any associated references are available in the online version of the paper at www.nature.com/nature.

Received 10 November; accepted 15 December 2008.
Published online 21 January 2009.

1. Meylan, E., Tschopp, J. & Karin, M. Intracellular pattern recognition receptors in the host response. *Nature* **442**, 39–44 (2006).

2. Ishii, K. J. *et al.* A Toll-like receptor-independent antiviral response induced by double-stranded B-form DNA. *Nature Immunol.* **7,** 40–48 (2006).
3. Stetson, D. B. & Medzhitov, R. Recognition of cytosolic DNA activates an IRF3-dependent innate immune response. *Immunity* **24,** 93–103 (2006).
4. Takaoka, A. *et al.* DAI (DLM-1/ZBP1) is a cytosolic DNA sensor and an activator of innate immune response. *Nature* **448,** 501–505 (2007).
5. Ishii, K. J. *et al.* TANK-binding kinase-1 delineates innate and adaptive immune responses to DNA vaccines. *Nature* **451,** 725–729 (2008).
6. Muruve, D. A. *et al.* The inflammasome recognizes cytosolic microbial and host DNA and triggers an innate immune response. *Nature* **452,** 103–107 (2008).
7. Hornung, V. *et al.* Silica crystals and aluminum salts activate the NALP3 inflammasome through phagosomal destabilization. *Nature Immunol.* **9,** 847–856 (2008).
8. Ludlow, L. E., Johnstone, R. W. & Clarke, C. J. The HIN-200 family: more than interferon-inducible genes? *Exp. Cell Res.* **308,** 1–17 (2005).
9. Ishii, K. J. & Akira, S. Innate immune recognition of, and regulation by, DNA. *Trends Immunol.* **27,** 525–532 (2006).
10. Manji, G. A. *et al.* PYPAF1, a PYRIN-containing Apaf1-like protein that assembles with ASC and regulates activation of NF-κB. *J. Biol. Chem.* **277,** 11570–11575 (2002).
11. Grenier, J. M. *et al.* Functional screening of five PYPAF family members identifies PYPAF5 as a novel regulator of NF-κB and caspase-1. *FEBS Lett.* **530,** 73–78 (2002).
12. Wang, L. *et al.* PYPAF7, a novel PYRIN-containing Apaf1-like protein that regulates activation of NF-κB and caspase-1-dependent cytokine processing. *J. Biol. Chem.* **277,** 29874–29880 (2002).
13. Finn, R., Griffiths-Jones, S. & Bateman, A. Identifying protein domains with the Pfam database. *Curr. Protoc. Bioinformatics* **Chapter 2,** Unit–2.5 (2003).
14. Albrecht, M., Choubey, D. & Lengauer, T. The HIN domain of IFI-200 proteins consists of two OB folds. *Biochem. Biophys. Res. Commun.* **327,** 679–687 (2005).
15. Landolfo, S., Gariglio, M., Gribaudo, G. & Lembo, D. The Ifi 200 genes: an emerging family of IFN-inducible genes. *Biochimie* **80,** 721–728 (1998).
16. Ding, Y. *et al.* Antitumor activity of IFIX, a novel interferon-inducible HIN-200 gene, in breast cancer. *Oncogene* **23,** 4556–4566 (2004).
17. Trapani, J. A. *et al.* A novel gene constitutively expressed in human lymphoid cells is inducible with interferon-γ in myeloid cells. *Immunogenetics* **36,** 369–376 (1992).
18. Burrus, G. R., Briggs, J. A. & Briggs, R. C. Characterization of the human myeloid cell nuclear differentiation antigen: relationship to interferon-inducible proteins. *J. Cell. Biochem.* **48,** 190–202 (1992).
19. DeYoung, K. L. *et al.* Cloning a novel member of the human interferon-inducible gene family associated with control of tumorigenicity in a model of human melanoma. *Oncogene* **15,** 453–457 (1997).
20. Yu, J. W. *et al.* Cryopyrin and pyrin activate caspase-1, but not NF-κB, via ASC oligomerization. *Cell Death Differ.* **13,** 236–249 (2006).
21. Szentesi, G. *et al.* Computer program for determining fluorescence resonance energy transfer efficiency from flow cytometric data on a cell-by-cell basis. *Comput. Methods Programs Biomed.* **75,** 201–211 (2004).
22. Henry, T. *et al.* Type I interferon signaling is required for activation of the inflammasome during *Francisella* infection. *J. Exp. Med.* **204,** 987–994 (2007).
23. Sun, K. H., Yu, C. L., Tang, S. J. & Sun, G. H. Monoclonal anti-double-stranded DNA autoantibody stimulates the expression and release of IL-1β, IL-6, IL-8, IL-10 and TNF-α from normal human mononuclear cells involving in the lupus pathogenesis. *Immunology* **99,** 352–360 (2000).
24. Schachman, H. K. *et al.* Enzymatic synthesis of deoxyribonucleic acid. VII. Synthesis of a polymer of deoxyadenylate and deoxythymidylate. *J. Biol. Chem.* **235,** 3242–3249 (1960).
25. Kanneganti, T. D. *et al.* Critical role for Cryopyrin/Nalp3 in activation of caspase-1 in response to viral infection and double-stranded RNA. *J. Biol. Chem.* **281,** 36560–36568 (2006).
26. Severa, M., Coccia, E. M. & Fitzgerald, K. A. Toll-like receptor-dependent and -independent viperin gene expression and counter-regulation by PRDI-binding factor-1/BLIMP1. *J. Biol. Chem.* **281,** 26188–26195 (2006).

Supplementary Information is linked to the online version of the paper at www.nature.com/nature.

Acknowledgements We would like to thank A. Cerny for animal husbandry and genotyping and R. Johnstone for the anti-AIM2 antibody. V.H. is supported by a fellowship from the Deutsche Forschungsgemeinschaft (German Research Foundation; Ho2783/2-1), E.L. and K.A.F. are supported by grants from the National Institutes of Health (AI-065483 (to E.L.) and AI-067497 (to K.A.F.)).

Author Contributions V.H. conceived the research and conducted the experiments with A.A., M.C.-D., F.B. and G.H. D.R.C. performed sequence analysis. E.L. and K.A.F. oversaw the whole project.

Author Information Reprints and permissions information is available at www.nature.com/reprints. Correspondence and requests for materials should be addressed to K.A.F. (kate.fitzgerald@umassmed.edu) or V.H. (veit.hornung@uni-bonn.de).

METHODS

Plasmid constructs. Full-length human AIM2 (1–356, on the basis of BC010940.1), AIM2-PYD (1–83), AIM2-HIN (148–356), IFIX (1–461, NM_198929), IFIX-PYD (1–84), IFI16 (1–729, NM_005531), IFI16-PYD (1–84), MNDA (1–407), MNDA-PYD (1–84, NM_002432) and NLRP3-PYD (1–87, NM_004895.3) were cloned by PCR from cDNA into pEFBOS-C-term-CFP using PCR-generated XhoI and BamHI or BglII restriction sites. AIM2 full-length, AIM2-PYD and AIM2-HIN were subcloned into pEFBOS-C-term-Flag/His using XhoI and BamHI. Murine pro-IL1β (1–269) was obtained by PCR from cDNA and fused into pEFBOS-C-term-GLuc/Flag using XhoI and BglII/BamHI. Expression plasmids (pCI) encoding human caspase-1 and ASC–HA were from Millenium Pharmaceuticals.

Reagents. ATP, LPS and poly(dA:dT) were from Sigma-Aldrich. A555-conjugated cholera-toxin B was from Molecular Probes, Invitrogen. DRAQ5 was from Biostatus. Biotinylated and FITC-labelled poly(dA:dT) were made by adding biotin-dUTP or FITC-dUTP (Fermentas) at a molar ratio of 1:8 to dTTP in the enzymatic synthesis of poly(dA:dT) as described[24]. Anthrax lethal toxin (anthrax protective antigen and lethal factor) was from List Biologicals). The anti-human-AIM2 antibody (3B10) was from R. Johnstone.

Mice. *Nlrp3*$^{-/-}$ and *Pycard*$^{-/-}$ mice were as previously described[25]. Both strains, as well as *Nlrp6*$^{-/-}$ and *Nlrp12*$^{-/-}$ mice were from Millennium Pharmaceuticals, and caspase-1-deficient mice were from R. Flavell. C57BL/6, 129/Sv, C57/BL6 × 129 F_1 and *Il1r1*$^{-/-}$ mice were from Jackson Laboratories. All mouse strains were bred and maintained under specific pathogen-free conditions in the animal facilities at the University of Massachusetts Medical School.

Sequence analysis. Pyrin-domain-containing sequences were retrieved from UniProt after identifying them in SMART. A multiple-sequence alignment of selected pyrin domains was generated using MUSCLE[27]. Secondary structure elements from the POP1 crystal structure (Protein Data Bank accession 2HM2) were mapped to the multiple-sequence alignment in PFAAT[28]. Prediction of nuclear targeting sequences and subcellular localization was done using PSORTII (http://psort.ims.u-tokyo.ac.jp/).

Cell culture and stimulation. Bone-marrow-derived macrophages were generated and cultured in DMEM medium as described[26]. THP-1 cells and macrophage cell lines were cultured as previously described[7]. One day before stimulation, THP-1 cells were differentiated using 0.5 μM PMA[7]. ATP (5 mM) was added 1 h before collection of supernatants. Poly(dA:dT) DNA and all other DNAs were transfected using Lipofectamine 2000 at a concentration of 1 μg ml^{-1} according to the manufacturer's instructions. Expression plasmids were transfected into 293T cells using GeneJuice (Novagen). Vaccinia virus (WR strain) was used for infection at a MOI of 5 if not indicated otherwise. Anthrax lethal toxin (protective antigen and lethal factor) were both at 5 μg ml^{-1}.

ELISA. Cell culture supernatants were assayed for IL1β by ELISA (BD Biosciences). To measure intracellular IL1β, cells were washed and subjected to three freeze-thaw cycles in assay diluent.

Confocal microscopy. Confocal microscopy was performed on a Leica SP2 AOBS confocal laser scanning microscope. Separation of CFP and YFP was performed using sequential scanning and 405 and 514 nm excitation.

Flow cytometry fluorescence resonance energy transfer. Three fluorescent intensities were measured: I1, direct excitation and emission of donor; I2, indirect excitation and direct emission of acceptor; and I3, direct excitation and emission of acceptor. After full correction for spectral bleed-through and cross excitation, FRET efficiency was calculated on a cell-by-cell basis[21] and then FRET efficiency histograms were plotted with GraphPad Prism 5.01 (GraphPad Software).

Immunoblot analysis. Immunoblotting was conducted as previously described[7] using anti-murine caspase-1 p10 (Santa Cruz Biotechnology), anti-Flag (M2, Sigma), anti-HA (Roche Applied Science), anti-CFP (Santa Cruz Biotechnology), anti-ASC (Alexis, AL177), anti-IFI16 (sc-8023, Santa Cruz Biotechnology) or anti-AIM2 (3B10 mouse IgG1[29]).

Co-immunoprecipitation assays. 293T cells (24 wells) were transfected with 1,550 ng of the PYD–CFP expression plasmids and 50 ng of ASC–HA. Twenty-four hours later, cell lysates were cleared by centrifugation (20,000*g*, 30 min) and subsequently incubated with anti-HA agarose beads for 2 h at 4 °C. Differentiated THP-1 cells were primed with Sendai virus (300 haemagglutinating units (HAU) ml^{-1}) overnight and subsequently lysed in high salt lysis buffer (250 mM NaCl, 10 mM Tris-HCl, pH 7.4, 1% CHAPS, protease inhibitor cocktail). Lysates were cleared by centrifugation, salt concentration was adjusted to 125 mM NaCl and ASC was immunopreciptated using rabbit polyclonal anti-ASC antibody. After six washes in both cases beads were boiled with Laemmli buffer for immunoblot analysis.

Quantitative real-time PCR. Quantitative rtPCR analysis was performed as described[26]. Primer sequences for murine *Hprt1*, *Ifnb*, *Aim2* and *Il6* are available upon request.

shRNA-mediated silencing. The lentiviral shRNA expression plasmids were from OpenBiosystems. The shRNAs targeting *Aim2* are: TRCN0000096104 (shRNA1), TRCN0000096105 (shRNA2) and TRCN0000096106 (shRNA3). The control shRNA is directed against murine *Ifih1* (TRCN0000103648) and was confirmed not to have any affect on *Nlrp3* or *Aim2* expression. The production of viral particles and transduction of target cells was conducted as described on http://www.broad.mit.edu/genome_bio/trc/publicProtocols.html.

AlphaScreen assay. The AlphaScreen was set up as an association assay. Proteins were transiently expressed in 293T cells and purified using Flag beads (Sigma) binding to the C-terminal Flag/His tag. The protein of interest was incubated at a concentration of 100 nM with biotinylated ligand at the indicated concentration in PBS, 0.1% BSA and 0.01% Tween 20 for 60 min. Subsequently, nickel chelate acceptor beads (binding to the His tag) and streptavidin-coated donor beads were added. After 30 min incubation at 25 °C in the dark, samples were read in proxiplates with the Envision HT microplate reader (all Perkin Elmer). Data were analysed by GraphPad Prism.

Reporter assays. All reporter gene assays were conducted as described[26].

siRNA transfection. Differentiated THP-1 cells were plated at 2.5 × 10^4 cells per well in 96-well plates and transfected with siRNA targeting human *AIM2* (sense strand: 5′-CCCGAAGATCAACACGCTTCA-3′), human *ASC* (sense strand: 5′-CGGGAAGGTCCTGACGGATGA-3′) or human *TLR8* (5′-GGGAGUUACUGCUUGAAG A-3′) using 275 ng siRNA and 0.75 μl Lipofectamine 2000. Cells were stimulated as indicated 48 h after transfection.

Cell viability assay. To quantify cell viability, macrophages (1 × 10^5 cells per well in 96-well plates) were treated as described. After 24 h, cells were washed with PBS and incubated in PBS plus 5 μM calcein AM (Invitrogen) for 30 min at 37 °C. The number of viable cells was assessed by counting fluorescent cells in two independent visual fields (×20 magnification) using ImageJ or by determining the overall fluorescence intensity using an Envision HT microplate reader.

27. Edgar, R. C. MUSCLE: multiple sequence alignment with high accuracy and high throughput. *Nucleic Acids Res.* **32,** 1792–1797 (2004).
28. Caffrey, D. R. *et al.* PFAAT version 2.0: a tool for editing, annotating, and analyzing multiple sequence alignments. *BMC Bioinformatics* **8,** 381 (2007).
29. Cresswell, K. S. *et al.* Biochemical and growth regulatory activities of the HIN-200 family member and putative tumor suppressor protein, AIM2. *Biochem. Biophys. Res. Commun.* **326,** 417–424 (2005).